Environmental Science & Technology

ARTICLE

pubs.acs.org/est

Effects of Cake Collapse Caused by Deposition of Fractal Aggregates on Pressure Drop during Ceramic Filtration

Wei Zhang,[*,†,‡] Cai-Ting Li,[*,†,‡] Xian-Xun Wei,[†,‡] Hong-Liang Gao,[†,‡] Qing-Bo Wen,[†,‡] Xiao-Peng Fan,[†,‡] Xin Shu,[†,‡] Guang-Ming Zeng,[†,‡] Wei Wei,[§] Yun-Bo Zhai,[†,‡] Yi-De He,[†,‡,∥] and Shan-Hong Li[†,‡]

[†]College of Environmental Science and Engineering, Hunan University, Changsha 410082, P.R. China

[‡]Key Laboratory of Environmental Biology and Pollution Control (Hunan University), Ministry of Education, Changsha 410082, P.R. China

[§]Guangzhou Hanhua Architects & Engineers Ltd, Guangzhou 510655, P.R. China

[∥]Department of Analytical and Environmental Chemistry, Humboldt University of Berlin, Berlin D-10099, Germany

Supporting Information

ABSTRACT: A cake collapse model was developed by taking the combined effects of fractal dimension, relaxation ratio, coordination number, and aggregate diameter into consideration. The cake porosity including intraaggregate and interaggregate porosities was modeled successively by three typical coordination numbers (n = 6, 8, and 12). Accordingly, an inversion method made it possible to deduce the coordination number using the measured cake porosities, and the reverse-calculated value with minimum error and the corresponding relaxation ratios were applied as the parameters for the model. As a result, the profiles of intraaggregate and interaggregate porosities and cake porosity were respectively predicted in contrast to the integrated variation of the relaxation ratio and the fractal dimension. Furthermore, a comparison between the model predictions of the cake pressure drop gradients with and without aggregate compression was conducted to validate the presence of cake collapse. The results show that the predictions based on the proposed collapse model are in agreement with the experiments, and the coordination number is one of the key factors that must be incorporated into the cake collapse models.

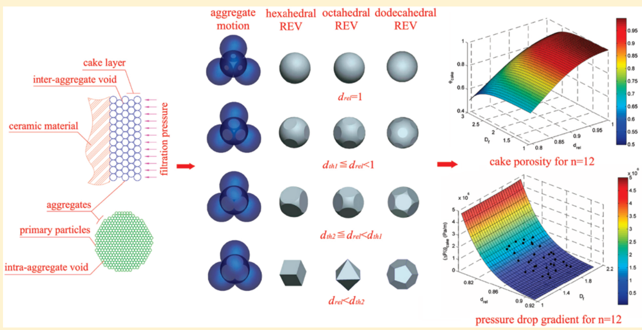

1. INTRODUCTION

Ceramic filters are widely utilized in dust removal because of high strength, high-temperature resistance, and corrosion resistance.[1,2] However, the pressure drop, one of the crucial filter parameters, is usually affected by the change of cake void fraction. Recent researches indicate that the cake layer is mainly formed by many aggregates composed of primary particles,[3−5] and the most dominating mechanism for aggregate formation is dependent on the particle bonds generated by particle cohesion and funicular-state bridges.[6−10] According to Xie's report,[11] the bond strength between particles of ca. 1−10 μm is ca. 10^4 Pa and that between aggregates of ca. 100 μm is only ca. 52 Pa. So, the aggregates cannot be turned into the larger aggregates and a cake layer is generally formed as a result of aggregate accumulation. Though there is somewhat of a deformation under the normal applied pressures of 2−5 kPa during filtration,[12] the bonds between particles will not be destroyed. Therefore, many investigators[13−15] employed aggregate theories to study the characteristics of the cake layer.

Because of the presence of aggregates, the change in the volume of compressed aggregates leads to cake collapse and consequently results in the change of pressure drop during filtration. To study the cake collapse, the fractal dimension of an aggregate and the center distance between two neighboring aggregates should be considered first. Many models are newly developed by considering the fractal dimension. For instance, Lee et al.[4] proposed an approach to calculate the values of fractal dimensions, Li et al.[16] developed two different fractal approaches to describe the aggregate permeability, and Park et al.[3] developed a cake collapse model by investigating the combined effect of the fractal dimension and the center distance on permeability of collapsed cake. Besides, coordination number, that is, the number of neighboring aggregates around an aggregate, is also an important variable for the cake porosity. Many investigators such as Skuazu et al.[17] and Georgalli et al.[18] provided the ways of estimating coordination number. Moreover, Tarbuck,[19] Rumpf,[20] and Shinohara[21] proposed some more convenient empirical formulas.

Received: December 2, 2010
Accepted: March 30, 2011
Revised: March 30, 2011
Published: April 13, 2011

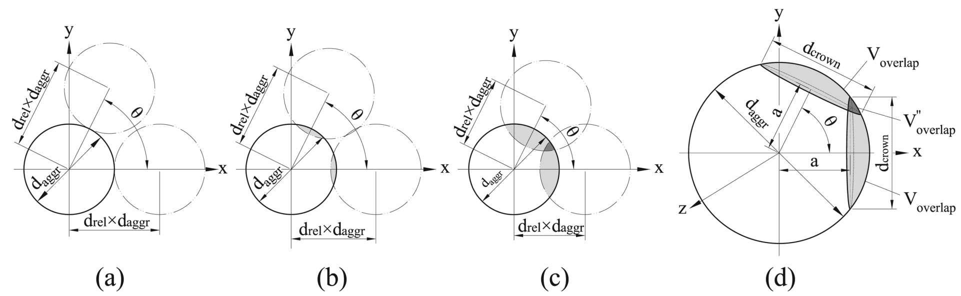

Figure 1. Schematic illustrations of the neighboring aggregates (a) without cake collapse, (b) with cake collapse for $d_{th1} < d_{rel} < 1$, (c) with cake collapse for $d_{rel} < d_{th2}$, (d) the overlapped regions.

To date, there has not been a report in the literature regarding the development of a mathematical model for the cake collapse with consideration of the combined effect of those variables on the cake pressure drop during filtration. Moreover, an effective method has not yet been developed to estimate coordination number and relaxation ratio because they are difficult to get merely by experiments.

In the present work, a mathematical model for predicting cake collapse during ceramic filtration was developed by regarding fractal dimension, relaxation ratio (related with center distance), coordination number, and aggregate diameter as model parameters. An inversion method was designed to accurately determine coordination number and relaxation ratio by using the measured cake porosities. In addition, a comparison between the proposed collapse model and the model without collapse was conducted to validate the presence of cake collapse with experiments.

2. MATHEMATICAL CALCULATIONS

Many aggregates with different sizes formed in the high-temperature flue gas by the bonds between carbonblack particles may deposit on the surface of a filter. Those aggregates with self-similar features can be assumed to be characterized by a single fractal dimension, D_f. The number of primary particles (N_P) within an aggregate of diameter d_{aggr} is related to its D_f as follows:[3,5,9]

$$N_P = c\left(\frac{d_{aggr}}{d_p}\right)^{D_f} \tag{1}$$

where d_p is the diameter of the primary particle, and c is the packing coefficient. Through the application of the box-counting dimension method for self-similar spheres, c was assumed to be 0.25, the same value used by previous studies.[16] To establish the cake collapse model with the uniform aggregates and particles, it is presumed that d_{aggr} and d_p are replaced by the equivalent mass mean diameters $\bar{d}_{aggr}$ and $\bar{d}_p$. Then, the intraaggregate porosity φ_{intra} is derived from eq 1:[16]

$$\varphi_{intra} = 1 - c\left(\frac{\bar{d}_{aggr}}{\bar{d}_p}\right)^{D_f - 3} \tag{2}$$

For the aggregates with fractal features, φ_{intra} is a function of the aggregate diameter and the values of D_f should be less than 3, otherwise, φ_{intra} is a constant ($\varphi_{intra} = 0.75$).

When a cake layer is formed, the change of interaggregate void should be taken into account due to the large volume fraction. Hence, it is essential to select an aggregate surrounded by n aggregates (n is coordination number) as the research object. The value of n mainly depends on the arrangement of neighboring aggregates, and Ridgway & Tarbuck,[19] Rumpf,[20] and Shinohara,[21] provided different empirical formulas for it:

$$\text{Ridgway \& Tarbuck}: \varphi_{inter,\,init} = 1.072 - 0.1193n + 0.0043n^2 \tag{3}$$

$$\text{Rumpf}: n = \frac{\pi}{\varphi_{inter,\,init}} \tag{4}$$

$$\text{Shinohara}: n = 20.01(1 - \varphi_{inter,\,init})^{1.741} \tag{5}$$

where $\varphi_{inter,init}$ is the initial interaggregate porosity without cake collapse.

On the basis of Park et al.'s presumptions[3] and Molerus's coordination number theory,[22] each aggregate contacts with the neighboring coordination aggregates without compression, and there exist three typical aggregate arrangements (n = 6, 8, and 12). With the utilization of those coordination numbers, the calculated values of $\varphi_{inter,init}$ are 0.4764, 0.3954, and 0.2595, respectively. In this study, however, the real value of n should be estimated using $\varphi_{inter,init}$. Taking a unit of cake comprising an aggregate as a representative element volume (REV), their geometrical appearances for n = 6, 8, and 12 are hexahedron, octahedron, and dodecahedron. The values of $\varphi_{inter,init}$ can be calculated by:[3]

$$\varphi_{inter,\,init} = 1 - \frac{V_{aggr}}{V_{rev,\,init}} \tag{6}$$

where $V_{rev,init}$ is the initial volume of a REV, and V_{aggr} is the volume of an aggregate.

If the cake collapse is neglected, the values of interaggregate porosities φ_{inter} should be equal to those of $\varphi_{inter,init}$. Considering the effect of cake collapse on φ_{inter}, assumptions are made that under filtration pressure, a plastic deformation would occur in aggregates, the contact points would develop into the increasing contact surfaces, and the center distances between two neighboring spherical aggregates would decrease from d_{aggr} to $d_{rel} \times d_{aggr}$ (d_{rel} is the relaxation ratio, that is, the center distance after cake collapse divided by that before cake collapse) (Figure 1). Also, n neighboring spherical aggregates are assumed to be uniformly distributed around an aggregate, the relative displacements caused by plastic deformations are assumed to be consistent, and the primary particles in the aggregates are regarded as the noncompressed particles. On the basis of the above assumptions, consequently, the values of φ_{inter} are actually less

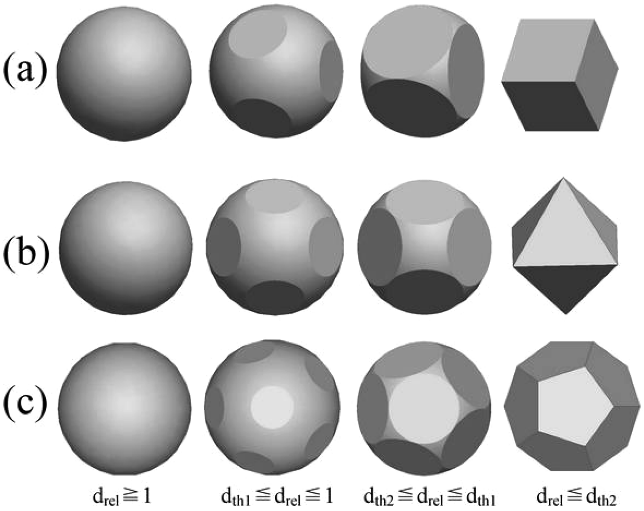

Figure 2. Appearances of aggregates with the packing structure of (a) hexahedron, (b) octahedron, (c) dodecahedron during cake collapse.

than those of $\varphi_{\mathrm{inter,init}}$ during filtration on account of the decrease of d_{rel}.

To study the change of φ_{inter}, the volume change of aggregates should be considered first. When d_{rel} is less than 1 and greater than a primary threshold value, two aggregates begin to interpenetrate into each other under filtration pressure, the aggregate surface consisting of the contact surfaces, and the remaining broken spherical surface is no longer a whole spherical surface, and an overlapped volume V_{overlap} will occur accordingly. As d_{rel} keeps decreasing until it is less than the primary threshold value and greater than a second threshold value, two neighboring overlapped parts begin to interpenetrate each other and an excessive overlapped volume V''_{overlap} will be yielded. When the value of d_{rel} is less than the second threshold value, the spherical surface of the aggregate is completely replaced by the contact surfaces, and the value of φ_{inter} would equal zero. The primary threshold value of d_{rel} is defined as d_{th1} when the V''_{overlap} occurs and the second threshold value of d_{rel} is defined as d_{th2} when each aggregate converts into a certain polyhedron (Figure 2). When the value of d_{rel} locates in the range from d_{th1} to 1, the expression of φ_{inter} should be revised by:

$$\varphi_{\mathrm{inter}} = 1 - \frac{V_{\mathrm{aggr}} - nV_{\mathrm{overlap}}}{V_{\mathrm{rev}}} \text{ for } d_{\mathrm{th1}} \le d_{\mathrm{rel}} < 1 \tag{7}$$

when the value of d_{rel} locates in the range from d_{th2} to d_{th1}, the expression of φ_{inter} should be revised by:

$$\varphi_{\mathrm{inter}} = 1 - \frac{V_{\mathrm{aggr}} - nV_{\mathrm{overlap}} + mV''_{\mathrm{overlap}}}{V_{\mathrm{rev}}} \text{ for } d_{\mathrm{th2}} < d_{\mathrm{rel}} < d_{\mathrm{th1}} \tag{8}$$

where m is the number of V''_{overlap}; when d_{rel} is less than d_{th2}, the value of φ_{inter} equals to zero. The geometric parameters of polyhedral REVs can be acquired by calculation (Supporting Information). The value of V_{overlap} is calculated by:

$$V_{\mathrm{overlap}} = \frac{\pi d_{\mathrm{aggr}}^3}{24}\left(d_{\mathrm{rel}}^3 - 3d_{\mathrm{rel}} + 2\right) \tag{9}$$

To calculate V''_{overlap}, the effects of n on the coordination angle θ must be taken into account (part d of Figure 1). For $d_{\mathrm{th2}} < d_{\mathrm{rel}} < d_{\mathrm{th1}}$, V''_{overlap} is calculated by:

$$V''_{\mathrm{overlap}} = \int_a^b \int_{f(x)}^{\sqrt{R^2 - x^2}} 2\sqrt{R^2 - x^2 - y^2}\,\mathrm{d}y\,\mathrm{d}x \tag{10}$$

where $R = d_{\mathrm{aggr}}/2$, $a = d_{\mathrm{rel}} d_{\mathrm{aggr}}/2$,

$$b|_{n=6} = \sqrt{R^2 - a^2}, f(x)|_{n=6} = \frac{d_{\mathrm{rel}} d_{\mathrm{aggr}}}{2}$$

$$\begin{aligned} b|_{n=8} &= 3.34 \times 10^{-1} a + 8.89 \\ &\quad \times 10^{-4}\sqrt{1.13 \times 10^6 (R^2 - a^2)}, \\ f(x)|_{n=8} &= -0.354x + 1.061a \end{aligned}$$

$$\begin{aligned} b|_{n=12} &= 4.46 \times 10^{-1} a + 1.60 \\ &\quad \times 10^{-4}\sqrt{3.12 \times 10^7 (R^2 - a^2)}, \\ f(x)|_{n=12} &= -0.499x + 1.117a \end{aligned}$$

For different coordination numbers, the values of V_{rev} are given by:

$$V_{\mathrm{rev}}|_{n=6} = 8a^3, V_{\mathrm{rev}}|_{n=8} = 6.93a^3, V_{\mathrm{rev}}|_{n=12} = 5.55a^3 \tag{11}$$

Combining eqs 7−11, the value of φ_{inter} can be obtained. Because the values of V_{aggr} are changed by cake collapse in a REV, eq 2 must be revised according to the variation of V_{aggr}:

$$\varphi_{\mathrm{intra}}^{\mathrm{real}} = \varphi_{\mathrm{intra}}(1 - \varphi_{\mathrm{inter}})\frac{V_{\mathrm{rev}}}{V_{\mathrm{aggr}}} \tag{12}$$

Using the calculated values of φ_{inter} and $\varphi_{\mathrm{intra}}^{\mathrm{real}}$, the cake porosity φ_{cake} can be expressed as:[3,23]

$$\varphi_{\mathrm{cake}} = 1 - (1 - \varphi_{\mathrm{intra}}^{\mathrm{real}})(1 - \varphi_{\mathrm{inter}}) \tag{13}$$

On the basis of the above analysis, the conventional cake filtration theory[24,25] can be utilized to calculate the total filter pressure drop, $\Delta P_{\mathrm{total}}$:

$$\Delta P_{\mathrm{total}} = \Delta P_{\mathrm{filter}} + \Delta P_{\mathrm{cake}} \tag{14}$$

where $\Delta P_{\mathrm{filter}}$ is the pressure drop of clean filter and ΔP_{cake} is the cake pressure drop, and they can be calculated by the Ergun equation:[26]

$$\Delta P_{\mathrm{filter}} = \delta_{\mathrm{filter}}\left(\frac{150\mu}{\bar{d}_{\mathrm{filter}}^2}\frac{(1 - \varphi_{\mathrm{filter}})^2}{\varphi_{\mathrm{filter}}^3}u_{\mathrm{f}} + \frac{1.75\rho}{\bar{d}_{\mathrm{filter}}}\frac{(1 - \varphi_{\mathrm{filter}})}{\varphi_{\mathrm{filter}}^3}u_{\mathrm{f}}^2\right)$$

$$\Delta P_{\mathrm{cake}} = \delta_{\mathrm{cake}}\left(\frac{150\mu}{\bar{d}_{\mathrm{p}}^2}\frac{(1 - \varphi_{\mathrm{cake}})^2}{\varphi_{\mathrm{cake}}^3}u_{\mathrm{f}} + \frac{1.75\rho}{\bar{d}_{\mathrm{p}}}\frac{(1 - \varphi_{\mathrm{cake}})}{\varphi_{\mathrm{cake}}^3}u_{\mathrm{f}}^2\right)$$

where δ_{filter} and δ_{cake} are the filter thickness and the cake layer thickness, $\bar{d}_{\mathrm{filter}}$ is the equivalent mean diameter of ceramic material, $\varphi_{\mathrm{filter}}$ is the filter porosity, ρ is the fluid density, μ is the dynamic fluid viscosity, u_{f} is the superficial fluid velocity. Although researchers have reported the thickness is uneven and porosity is heterogeneous in the cake layer,[25,27] the assumptions of uniform cake thickness and porosity are employed to simplify calculation in this model.

Table 1. Prediction of d_{rel} and n for Aggregates by Comparing the Cake Porosities Calculated by the Model Equations with the Experimental Values

		φ_{cake}				MSE		
D_f	d_{rel}	$n = 6$	$n = 8$	$n = 12$	$\varphi_{cake,test}$	$n = 6$	$n = 8$	$n = 12$
1.74	0.809	0.670	0.809	0.701	0.718	0.0339	0.0643	0.0120
1.64	0.875	0.951	0.937	0.874	0.868	0.0587	0.0488	0.0042
1.88	0.835	0.919	0.866	0.769	0.774	0.1025	0.0651	0.0035
1.83	0.824	0.894	0.848	0.742	0.753	0.0997	0.0672	0.0078
1.91	0.834	0.907	0.960	0.765	0.747	0.1131	0.1506	0.0127
1.87	0.831	0.901	0.849	0.757	0.776	0.0884	0.0516	0.0134
1.93	0.823	0.886	0.845	0.732	0.721	0.1167	0.0877	0.0078

3. MATERIALS AND METHODS

Primary Particle and Aggregate. The equivalent mean diameter of the primary particles in the aggregates can be acquired by fitting the particle size distribution tested by a BT-9300H laser particle size analyzer (Bettersize Instruments Ltd., China) (Supporting Information). Additionally, the equivalent mean diameter of the aggregates can be obtained by statistically analyzing the micrographics, taken by a JSM-6700F Field Emission Scanning Electron Microscope (FE-SEM) (Japan Electron Optics Laboratory Ltd. Corp) using *Image Structure Analyzer in 3-Dimensions* software (Supporting Information).

Fractal Dimension. Using the box-counting dimension method,[28] the values of D_f were estimated from the fitting logarithmic pixel values of the micrographics, taken by the aforementioned FE-SEM (Supporting Information).

Relaxation Ratio and Coordination Number. Researches on d_{rel} and n were carried out in a specially designed suction filtration system. First, the true cake density and the bulk cake densities before and after cake collapse were measured. Then, the cake porosity $\varphi_{cake,test}$ before and after cake collapse can be determined from the measured true and bulk densities. Finally, the real value of n and the corresponding values of d_{rel} can be obtained by an inversion method (Supporting Information).

Filter Pressure Drop. To acquire the pressure drop of the suction filtration system, the vacuum degrees recorded by a vacuum meter were applied to calculate the corresponding pressure drop (Supporting Information). For the propose of acquiring the pressure drop of the ceramic filter, a SYT-2000 V digital pressure gauge (Shanghai Guigu Instruments Co., Ltd., China) was utilized to record the data directly (Supporting Information).

4. RESULTS AND DISCUSSION

Prediction of n and d_{rel} for Aggregates. An inversion method was designed to estimate the real value of n and the corresponding values of d_{rel}. First of all, the corresponding tables were constituted, which were the calculated values of φ_{cake} and φ_{inter} in contrast to the arbitrary variables of d_{rel} and D_f. Then, the values of $\varphi_{cake,test}$ were matched with those of φ_{cake} in the $\varphi_{cake}-D_f-d_{rel}$ tables to find the values of d_{rel}. Following that, the values of φ_{inter} could thereby be found in the $\varphi_{inter}-d_{rel}$ tables via the acquired d_{rel}. Because φ_{inter} is different with $\varphi_{inter,init}$ owning to cake collapse, $\varphi_{inter,init}$ should be gained based on φ_{inter} to deduce n by the formulas reported by literatures.[23−25] Finally, the value of n with minimum error and the corresponding values of d_{rel} were applied as parameters for this model (Supporting Information). To validate the resulting value of n, a comparison between the estimated and experimental cake porosities for various coordination numbers was performed (Table 1). As a result, the mean square errors (MSEs) for n = 6, 8, and 12, were calculated to express the difference between model estimations and experiments. The comparison shows the mean value of the MSEs for $n = 12$ is 8.77×10^{-3}, which is only approximately 10% of the mean MSE for $n = 6$, and 11.5% of the mean MSE for $n = 8$. It implies that when the carbonblack of $\bar{d}_p = 2.34\ \mu$m is employed as the primary particles, the value of n equal to 12 was more reasonable than other n values (n = 6 or 8) for the prediction of cake porosity and the corresponding values of d_{rel} for $n = 12$ was involved in the Supporting Information.

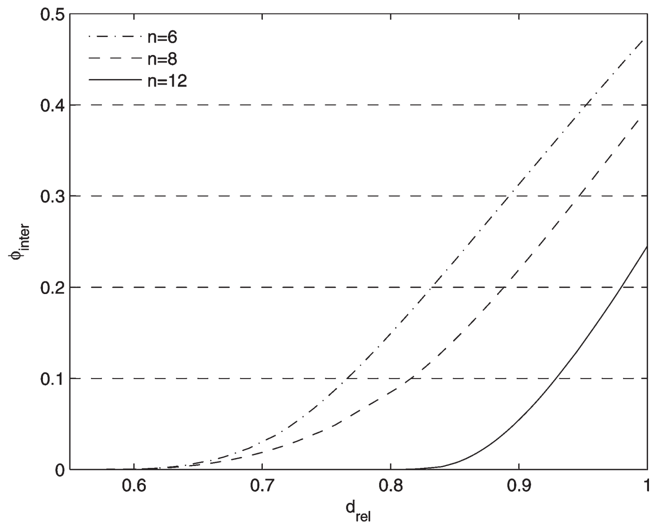

Figure 3. Predicted values of φ_{inter} as functions of d_{rel} for n = 6, 8, and 12.

Dependence of φ_{inter}, φ_{intra}^{real}, and φ_{cake} upon d_{rel} and D_f for Different Coordination Numbers. Figure 3 depicts the profiles of φ_{inter} with d_{rel} for n = 6, 8, and 12. From observation, the values of φ_{inter} decrease with the decrease of d_{rel} and the increase of n. Before collapse occurs ($d_{rel} = 1$) $\varphi_{inter} = \varphi_{inter,init}$, and after the aggregates completely develop into polyhedrons ($d_{rel} \le d_{th2}$) $\varphi_{inter} = 0$. Hence, the values of φ_{inter} mainly vary in the function range of $0 < \varphi_{inter} < \varphi_{inter,init}$ in contrast to the variable range of $d_{th2} < d_{rel} < 1$. When the values of d_{rel} locate in the range of $d_{th1} < d_{rel} < 1$, the values of φ_{inter} decrease sharply with cake collapse because the interaggregate voids shrinks due to the plastic deformation caused by the ever-increasing values of $V_{overlap}$. When $d_{th2} < d_{rel} < d_{th1}$, the values of φ_{inter} decrease slowly with cake collapse because $V_{overlap}$ is partly offset due to the occurrence of $V''_{overlap}$. For example, when the measured value of d_{rel} is 0.875, φ_{inter} is ca. 0.05 for $n = 12$ and it corresponds to an approximate 80.7% reduction compared to the initial value 0.2595.

Through the analysis of eqs 2−12, it is found that φ_{intra}^{real} is mainly affected by D_f, d_{aggr}, and d_{rel}. The calculated result suggests the value of φ_{intra}^{real} is rarely influenced by the aggregates of over ca. 50 μm (Supporting Information) and Park et al[3] have reported similar findings. Since the size of most of the observed aggregates is in the range of 50−150 μm (Supporting Information), only D_f and d_{rel} need to be taken into consideration for surveying the profiles of φ_{intra}^{real}. Figure 4 displays the dependence of φ_{intra}^{real} upon d_{rel} for n = 6, 8, and 12 under the condition that D_f is 1.74 and d_{aggr} is 97 μm. It is evident that the values of

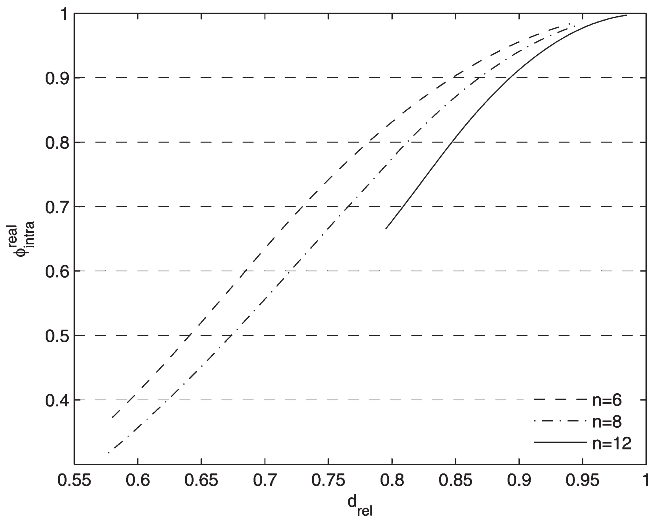

Figure 4. Predicted values of $\varphi_{\text{intra}}^{\text{real}}$ as functions of d_{rel} for $n = 6, 8$, and 12 under the condition of $D_f = 1.74$ and $d_{\text{aggr}} = 97\ \mu$m.

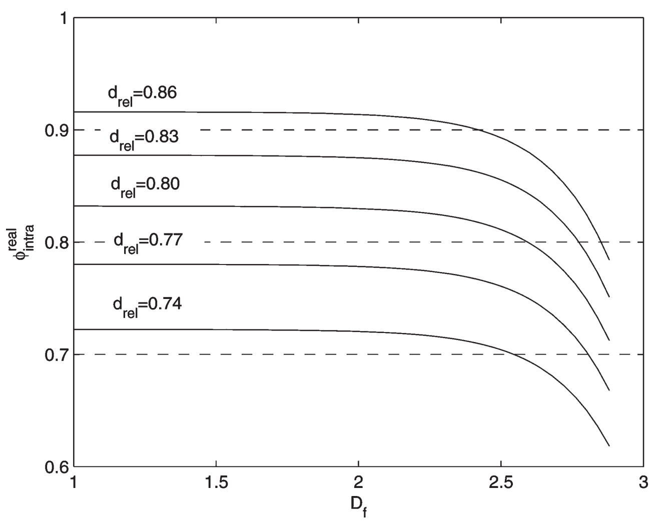

Figure 5. Predicted values of $\varphi_{\text{intra}}^{\text{real}}$ as functions of D_f at different relaxation ratios for $d_{\text{aggr}} = 97\ \mu$m and $n = 12$.

$\varphi_{\text{intra}}^{\text{real}}$ decrease with the decrease of d_{rel} and the increase of n. This indicates that cake collapse would reduce the values of $\varphi_{\text{intra}}^{\text{real}}$ because the values of φ_{inter} utilized for revising the values of φ_{intra} decrease with the decrease of d_{rel}. For instance, when d_{rel} decreases from 1 to 0.809, the reduced values of $\varphi_{\text{intra}}^{\text{real}}$ are 0.152, 0.209, and 0.322 for $n = 6$, 8, and 12, and the reductions are ca. 15%, 21%, and 32%, respectively. This finding implies that an aggregate with a greater value of n is more influenced by cake collapse. Through the analysis of Figures 3 and 4, it is also found that the values of φ_{inter} and $\varphi_{\text{intra}}^{\text{real}}$ decrease synchronously with the decrease of d_{rel}, resulting in a sharp decrease of φ_{cake}. In the context of cake collapse, the contribution of $\varphi_{\text{intra}}^{\text{real}}$ to φ_{cake} is more remarkable compared with φ_{inter}.

Additionally, $\varphi_{\text{intra}}^{\text{real}}$ was calculated as a function of D_f at different values of d_{rel} (Figure 5). The results show that, under the low value range of D_f, the values of $\varphi_{\text{intra}}^{\text{real}}$ of the aggregates are inclined to be a constant. However, under the high value range of D_f, the values of $\varphi_{\text{intra}}^{\text{real}}$ decrease rapidly while D_f increases.

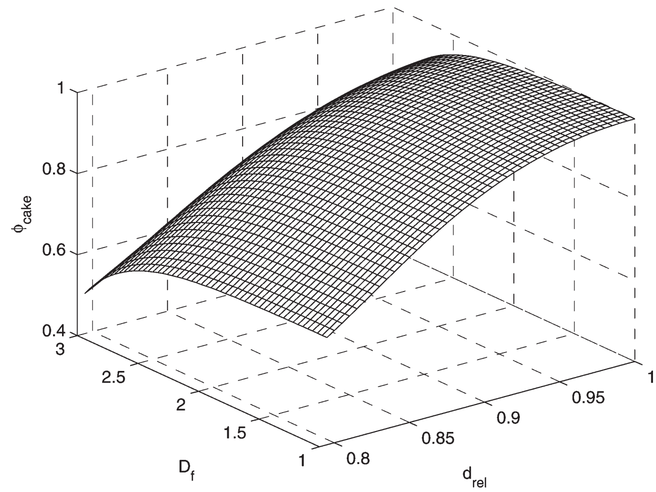

Figure 6. Predicted values of φ_{cake} as functions of D_f and d_{rel} of the aggregates for $n = 12$ and $d_{\text{aggr}} = 97\ \mu$m.

Table 2. Comparison of Cake Porosities Estimated by the Model Equations with the Experimental Values Measured by Two Different Filtration System for n = 12

D_f	d_{rel}	$\varphi_{\text{cake,model}}$	$\varphi_{\text{cake,test}}$	MSE
[a]2.36	0.812	0.701	0.724	0.0166
[a]2.52	0.827	0.729	0.730	0.0006
[a]2.44	0.831	0.742	0.744	0.0012
[a]2.49	0.818	0.707	0.728	0.0146
[b]1.67	0.896	0.908	0.920	0.0084
[b]1.72	0.913	0.937	0.955	0.0124
[b]1.94	0.922	0.947	0.957	0.0071
[b]1.78	0.931	0.961	0.961	0.0003

[a] Obtained in suction filtration system at superficial velocity 1 L/s, pressure drop of system 13 KPa, cake thickness 8 mm for 30 min. [b] Obtained in ceramic filter at superficial velocity 1.14 m/min, pressure drop of system 6.8 KPa, ambient concentration of suspension 7.687 g/m^3 for 120 min.

Comparing Figure 5 with Figure 4, it is evident that the effect of D_f on $\varphi_{\text{intra}}^{\text{real}}$ is less than that of d_{rel}.

Figure 6 shows a parametric surface of φ_{cake} specified by D_f and d_{rel} for $d_{\text{aggr}} = 97\ \mu$m and $n = 12$ (acquired by reverse-calculation using carbonblack particles). Combining the two variables, the reductions of φ_{cake} during cake collapse are mainly caused by the decrease of d_{rel} and the increase of D_f under the high dimension range, and the change of d_{rel} shows more effect on φ_{cake} than that of D_f.

The porosity model was verified with experiments using the suction filtration system and the ceramic filter, respectively (Table 2). First, the values of D_f were measured from the FE-SEM micrographics and the d_{rel} and n were estimated using the aforementioned method. Subsequently, the cake porosities for different values of n were predicted by the current variables. Finally, the MSEs were obtained by comparing the predicted and experimental values of cake porosity. The results show that the mean MSEs of experimental data tested from suction filtration system and ceramic filter are 8.3 × 10^{-3} and 7.1 × 10^{-3} respectively indicating that all of the values of φ_{cake} agree well with the values of $\varphi_{\text{cake,test}}$. It is also found that, when the suction filtration system was

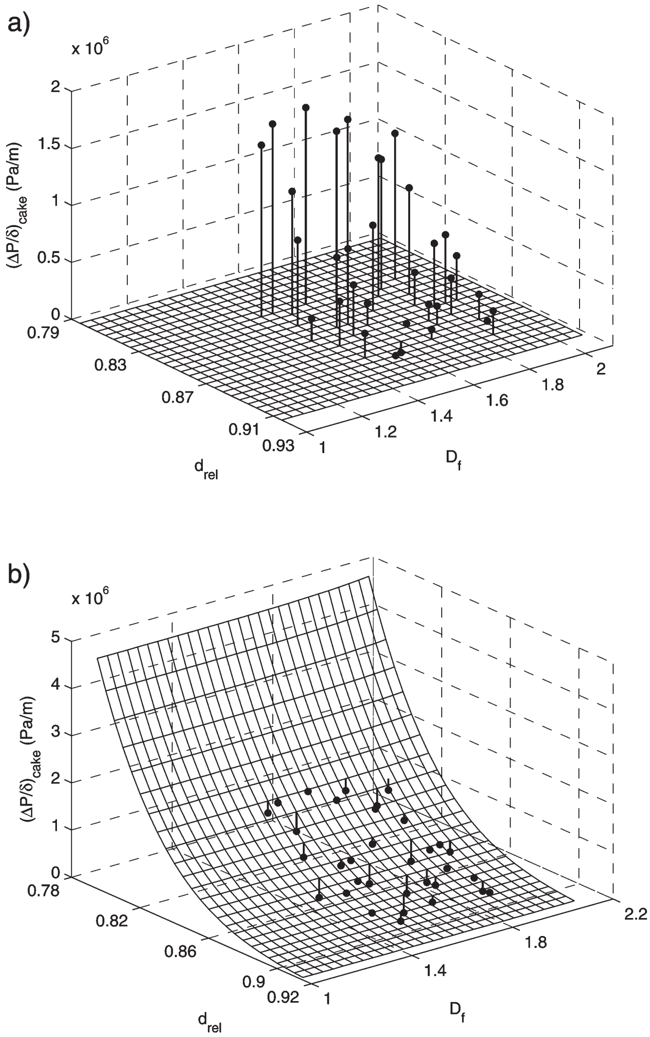

Figure 7. Comparison between predicted values of $(\Delta P/\delta)_{\mathrm{cake}}$ as functions of D_f and d_{rel} and experimental data (a) without (b) with consideration of cake collapse.

employed, the values of D_f were located in the region of higher values. And when ceramic filter was used, the values of D_f were in the range of lower values. This phenomenon illustrates that higher pressure can also increase D_f and decrease d_{rel}.

Consequently, this model can accurately predict the dependence of φ_{inter}, $\varphi_{\mathrm{intra}}^{\mathrm{real}}$ and φ_{cake} upon d_{rel} and D_f when the appropriate coordination number and the corresponding the values of d_{rel} are determined by reverse calculation. Furthermore, a conclusion could be made that the reduced φ_{cake} can increase the pressure drop, and the increased pressure drop can in turn reduce the value of φ_{cake}.

Effect of Cake Collapse on $(\Delta P/\delta)_{\mathrm{cake}}$. Through eqs 2−14, the effects of cake collapse on the cake pressure drop gradient $(\Delta P/\delta)_{\mathrm{cake}}$ were predicted by utilizing D_f and d_{rel} as variables. Part a of Figure 7 displays the parametric surface of $(\Delta P/\delta)_{\mathrm{cake}}$ specified by D_f and d_{rel} without cake collapse, that is, by setting d_{rel} to 1 in the model. It is evident that, if ignoring cake collapse, the calculated values are less influenced by d_{rel}. Simultaneously, the pressure gradient is barely affected by D_f. Even for relatively larger values of D_f, the pressure gradient remains relatively small (e.g., $(\Delta P/\delta)_{\mathrm{cake}} = 2794$ Pa/m for $D_f = 2.44$ and $d_{\mathrm{rel}} = 1$). Performing a comparison between the predictions and the experiments, the mean MSE is ca. 4.48×10^5 Pa/m. Part b of Figure 7 displays the parametric surface of $(\Delta P/\delta)_{\mathrm{cake}}$ specified by D_f and d_{rel} with cake collapse, that is, by setting the values of d_{rel} to the values between d_{th2} and 1 in the model. It is evident that the values of $(\Delta P/\delta)_{\mathrm{cake}}$ rapidly increase with the decrease of d_{rel}. In comparison with the results presented in part a of Figure 7, the predicted values with cake collapse are more dependent on d_{rel}, and the corresponding mean MSE is ca. 1.32×10^5 Pa/m, that is, ca. 29% of the mean MSE for part a of Figure 7. The further discussions on the predictions of the cake pressure drop were involved in the Supporting Information.

The findings in this work emphasize the importance of cake collapse to the pressure drop during ceramic filtration. In addition to relaxation ratio, fractal dimension, and aggregate size, the coordination number is also an important factor of the change of cake porosity. The unknown coordination number and the corresponding relaxation ratios can be obtained by an original inversion method when the measured porosities are employed as the inputs. On the basis of the comparison between predictions and experiments, the proposed model was proven to be considerably effective. Hence, this model has great application potential on the prediction of cake pressure drop because of high accuracy and convenient calculation.

■ ASSOCIATED CONTENT

S Supporting Information. Suction filtration, ceramic filtration, size distribution of primary particles, microscopic feature, and fractal dimensions of aggregates, parametric surfaces of φ_{cake} for $n = 6$ and 8, profiles of φ_{cake} with d_{aggr} for $n = 12$, validation of aggregates, validation of pressure drop, inversion method, and the nomenclature. This material is available free of charge via the Internet at http://pubs.acs.org.

■ AUTHOR INFORMATION

Corresponding Author

*Phone: +86 731 88649216, fax: +86 731 88649216, e-mail: ctli3@yahoo.com (C.-T.L.); wei_zhang@hnu.edu.cn. (W.Z.).

■ ACKNOWLEDGMENT

The authors are grateful for the financial support provided by the Natural Science Foundation of China (No. 50878080, 51039001 and 50908080), the Scientific and Technological Major Special Project of Hunan Province in China (2010XK6003), and the Fundamental Research Funds for the Central Universities in China.

■ REFERENCES

(1) Kim, J. H.; Liang, Y.; Sakong, K. M.; Choi, J. H.; Bak, Y. C. Temperature effect on the pressure drop across the cake of coal gasification ash formed on a ceramic filter. *Powder Technol.* **2008**, *181* (1), 67–73.

(2) LI, C. T.; Zhang, W.; W, X. X.; Gao, H. L.; Wen, Q. B.; Fan, X. P.; Liu, H.; Shu, X.; Wei, W. Experiment and simulation of micron-particles diffusion in porous ceramic vessel. *Trans. Nonferrous Met. Soc. China.* **2010**, *20* (12), 2358–2365.

(3) Park, P. K.; Lee, C. H.; Lee, S. Permeability of Collapsed Cakes Formed by Deposition of Fractal Aggregates upon Membrane Filtration. *Environ. Sci. Technol.* **2006**, *40* (8), 2699–2705.

(4) Lee, C.; Kramer, T. A. Prediction of three-dimensional fractal dimensions using the two-dimensional properties of fractal aggregates. *Adv. Colloid Interface Sci.* **2004**, *112* (1−3), 49–57.

(5) Veerapaneni, S.; Wiesner, M. R. Hydrodynamics of fractal aggregates with radially varying permeability. *J. Colloid Interface Sci.* **1996**, *177*, 45–57.
(6) Zebel, G. *Coagulation of aerosols in aerosol science*. Academic Press Inc.: New York, 1966.
(7) Fuchs, N. A. *The Mechanics of Aerosols*. The Macmillan Company: New York; Pergamon Press, Inc.: New York, 1964.
(8) Dennis, R. *Handbook on Aerosols*. A-energy Press Inc.: New York, 1976.
(9) Cleaver, J. A. S.; Karatzas, G.; Louis, S.; Hayati, I. Moisture-induced caking of boric acid powder. *Powder Technol.* **2004**, *146* (1−2), 93–101.
(10) Willett, C. D.; Adams, M. J.; Johnson, S. A;Capillary bridges between two spherical bodies. *Langmuir* **2000**, *16*, 9396–9405.
(11) Xie, H. Y. The role of interparticle forces in the fluidization of fine particles. *Powder Technol.* **1997**, *94*, 99–108.
(12) Neiva, A. C. B.; Goldstein, L., Jr. A procedure for calculating pressure drop during the build-up of dust filter cakes. *Chem. Eng. Process.* **2003**, *42*, 495–501.
(13) Bushell, G. C.; Yan, Y. D.; Woodfield, D.; Raper, J.; Amal, R. On techniques for the measurement of the mass fractal dimension of aggregates. *Adv. Colloid Interface Sci.* **2002**, *95*, 1–50.
(14) Li, X. Y.; Logan, B. E. Collision frequencies of fractal aggregates with small particles by differential sedimentation. *Environ. Sci. Technol.* **1997**, *31*, 1229–1236.
(15) Li, X. Y.; Logan, B. E. Collision frequencies of fractal aggregates with small particles by turbulent fluid shear. *Environ. Sci. Technol.* **1997**, *31*, 1237–1244.
(16) Li, X. Y.; Logan, B. E. Permeability of fractal aggregates. *Water Res.* **2001**, *35*, 3373–3380.
(17) Suzuki, M.; Kada, H.; Hirota, M. Effect of size distribution on the relation between coordination number and porosity of spheres in a randomly packed bed. *Adv. Powder Technol.* **1999**, *10* (4), 353–365.
(18) Georgalli, G. A.; Reuter, M. A. Modelling the co-ordination number of a packed bed of spheres with distributed sizes using a CT scanner. *Miner. Eng.* **2006**, *19* (3), 246–255.
(19) Rumpf, H. Physical aspects of comminution and new formulation of a law of comminution. *Powder Technol.* **1973**, *7* (3), 145–159.
(20) Shibata, H.; Mada, J.; Funatsu, K. Prediction of drying rate curves on sintered spheres of glass beads in superheated steam under vacuum. *Ind. Eng. Chem. Res.* **1990**, *29* (4), 614–617.
(21) Arakawa; Nishino. Contact number and porosity in randomly packed sphere mixtures of various sizes. *J. Sco. Mat. Sci. Japan.* **1973**, *22*, 658–662.
(22) Molerus, O. *Principles of Flow in Disperse Systems*; Chapman & Hall: London, U.K., 1993.
(23) Hwang, K. J.; Liu, H. C. Cross-flow microfiltration of aggregated submicron particles. *J. Membr. Sci.* **2002**, *201*, 137–148.
(24) Ju, J.; Chiu, M. S.; Tien, Chi. Further work on pulse-jet fabric filtration modeling. *Powder Technol.* **2001**, *118* (1−2), 79–89.
(25) Dittler, A.; Ferer, M. V.; Mathur, P.; Djuranovic, P.; Kasper, G.; Smith, D. H. Patchy cleaning of rigid gas filters-transient regeneration phenomena comparison of modelling to experiment. *Powder Technol.* **2002**, *124* (1−2), 55–66.
(26) Ergun, S. Fluid flow through packed columns. *Chem. Eng. Prog.* **1952**, *48*, 89–94.
(27) Ju, J.; Chiu, M. S.; Tien, C. Multiple-Objective Based Model Predictive Control of Pulse Jet Fabric Filters. *Chem. Eng. Res. Des.* **2000**, *78* (4), 581–589.
(28) Li, J.; Du, Q.; Sun, C. An improved box-counting method for image fractal dimension estimation. *Pattern Recogn.* **2009**, *42* (11), 2460–2469.